International Journal of Heat and Mass Transfer 51 (2008) 5872–5876

Contents lists available at ScienceDirect

International Journal of Heat and Mass Transfer

journal homepage: www.elsevier.com/locate/ijhmt

Dynamics of water sorption on a single adsorbent grain caused by a large pressure jump: Modeling of coupled heat and mass transfer

B.N. Okunev [a,*], A.P. Gromov [a], L.I. Heifets [a], Yu.I. Aristov [b]

[a] Moscow State University, Chemical Department, Vorobievi Gori, Moscow, Russia
[b] Boreskov Institute of Catalysis, Pr. Lavrentieva, 5, Novosibirsk 630090, Russia

ARTICLE INFO

Article history:
Received 4 January 2008
Received in revised form 19 January 2008
Available online 20 May 2008

Keywords:
Mathematical modeling
Coupled heat and mass transfer
Adsorption kinetics
Selective water sorbent
Adsorption heat pumps

ABSTRACT

Here we present a mathematical model of coupled heat and mass transfer in the course of water adsorption on a single adsorbent grain, which is in thermal contact with an isothermal metal plate. Adsorption is caused by a large jump of vapour pressure over the grain. The radial profiles of the grain temperature and the water concentrations in the adsorbed and gas phases were calculated as a function of time. Strong interrelationship between the shapes of the water sorption isotherm and the radial uptake profile was revealed. The best fit to the experimental data of [B. Dawoud, Yu. I. Aristov, Experimental study on the kinetics of water vapour sorption on selective water sorbents, silica–gels and alumina under typical operating conditions of sorption heat pumps, Int. J. Heat Mass Transfer 46 (2) (2003) 273–281] corresponds to the water diffusivity $D_e = 6.0 \times 10^{-6}$ m^2/s and the coefficient of the heat transfer $\alpha_p = 70$ W/(m^2 K) which are larger than those measured in quasi-equilibrium experiments.

1. Introduction

A new methodology of studying the kinetics of water vapour adsorption/desorption under operating conditions typical for isobaric stages of adsorption heat pumps (AHP) has been proposed and tested experimentally in [1]. The measurements have been carried out on loose pellets of composite adsorbent SWS-1L ($CaCl_2$ in silica KSK) placed on a metal plate. The temperature of the plate was changed as it takes place in real sorption heat pumps, while the vapour pressure over the adsorbent was maintained almost constant (saturation pressures corresponding to evaporator temperatures of 5 and 10 °C and condenser temperatures of 30 and 35 °C). The quasi-exponential behaviour of water uptake on time was found for most of the experimental runs. The characteristic time τ of isobaric adsorption (desorption) was measured for one layer of loose 1.4–1.6 mm grains for different boundary conditions of adsorption heat pumps. This approach allows a direct measurement of the temporal evolution of average water uptake under the conditions, which closely simulate the scenario of temperature jump or drop in real AHPs with a layer of loose grains. Such jump is a driving force of water desorption/adsorption during the isobaric stages of AHP cycle.

A dynamic model of the water vapour adsorption on a single adsorbent grain being in thermal contact with a metal plate subjected to a fast temperature jump/drop at almost constant vapour pressure was presented in [2]. The model took into account coupled heat and mass transfer in the grain coupled with adsorption processes. This model was used to analyze the experimental results presented in [1] and to study the links between dynamic and equilibrium parameters of the adsorption process. The temporal evolution of the average pressure P_{av} inside the grain, its average temperature T_{av} and uptake w were calculated. The uptake was found to be a quasi-exponential function of time as was observed in [1]. The characteristic times τ of isobaric adsorption/desorption calculated for a single grain of SWS-1L were in good agreement with those measured experimentally. The best fit corresponded to the water diffusivity $D_e = 3.0 \times 10^{-6}$ m^2/s and the coefficient of heat transfer between the plate and the grain $\alpha_p = 60$ W/(m^2 K). This diffusivity is very close to the Knudsen diffusivity in a straight cylindrical pore of radius $r_p = 7.5$ nm [4] at $T = 90$ °C = 363 K: $D_{kn} = 9700 \times r_p\sqrt{T/M} = 3.3 \cdot 10^{-6}$ m^2/s. The obtained efficient coefficient of heat transfer α_p was higher than the one theoretically estimated in [2]. These quite high values of D_e and α_p indicated that under essentially non-equilibrium conditions caused by the large temperature jump the transfer of both heat and vapour can be more efficient than under quasi-equilibrium conditions. Although the accordance of experimental and calculated data was good on the whole, the model failed in describing S-shaped parts of the kinetic curves recorded within the first dozens of seconds. This could be because in those experiments the temperature of the metal support reached the final value not in a trice but in some 20–50 s. On

* Corresponding author. Tel.: +7 495 939 46 49; fax: +7 495 939 33 16.
E-mail address: okunev@tech.chem.msu.ru (B.N. Okunev).

0017-9310/$ - see front matter © 2008 Elsevier Ltd. All rights reserved.
doi:10.1016/j.ijheatmasstransfer.2008.01.037

Nomenclature

D_e	efficient water diffusivity (m^2/s)
ΔH	heat of adsorption (J/mole)
m	mass (mole)
N	uptake ($mole_{H_2O}/mole_{CaCl_2}$)
P	pressure (mbar)
R_p	grain radius (m)
R	universal gas constant (J/mol K)
s	area of the hole between the reservoirs (m^2)
t	time (s)
T	temperature (K)
V	volume (m^3)
x	weight fraction of the salt (kg/kg)

Greek symbols

α_p	coefficient of heat transfer (W/m^2 K)
ε	grain porosity
χ	dimensionless adsorption
λ	coefficient of heat conductivity of the grain (W/m K)

Subscripts

av	average
w	water
0	initial value

the opposite, the model assumed a step-wise T-jump, which can not be attainable in real experiments due to the finite heat capacity of the support.

In [3] the dynamics of water sorption was studied for the same configuration of loose grains in a constant volume – variable pressure unit with a substantial difference that the driving force for water sorption was a pressure jump. The set-up consisted of two reservoirs: the buffering reservoir of 23.726 dm^3 volume contained the vapour at $P_1 = 60$ mbar and $T = 50$ °C, and the measuring cell of 0.732 dm^3 volume was maintained at $P_2 = 0.02$ mbar and $T = 50$ °C. At the beginning of the experiments the loose grains of SWS-1L were almost completely dry (residual uptake $x_0 = 0.0017$ g/g) and were maintained at the metal support temperature 50 °C. At $t = 0$ the reservoirs were connected and the pressure in the whole volume became equalized within less then 1 s [3]. After that the vapour pressure was decreasing due to the water sorption by the SWS grains. When measuring the temporal evolution of pressure $P(t)$, the time variation of the water loading was calculated. The adsorption process lasted some tens of minutes until the equilibrium was reached. The uptake change during the adsorption was as much as $\Delta N = 4.3$ mole H_2O per 1 mole $CaCl_2$ (or 0.24 g H_2O/g $CaCl_2$). As the pressure jump was large and the pressure was not constant during the water adsorption, no simple kinetic models could be applied for extracting kinetic parameters from the experimental curves. Later, the similar test rig was developed in [4] with the addition of a heat flux meter to measure the released heat of adsorption.

Mathematical modeling of the P-jump kinetic curves can likely ensure better conformity between model assumptions and experimental conditions than it could be accessible for the T-jump experiments. Although the mathematical modeling of both isothermal and non-isothermal adsorption on a single adsorbent grain has been performed in many papers [5–10] and summarized in [5], a complex hydrodynamic problem of simultaneous gas icicle (discharge) and sinking (generating) has not been analyzed yet. The aim of this work was a development of the model of the coupled heat and mass transfer in the course of water adsorption on a single adsorbent grain under the conditions described in [3]. The radial profile of the grain temperature and the water concentrations will be calculated as a function of time along with the temporal evolution of the average uptake. Calculated uptake curve will be compared with the experimental ones to estimate the efficient values of the water diffusivity D_e and the coefficient of the heat transfer α_p.

2. Description of the model

The model bears on the assumptions of the local adsorption equilibrium as well as the local equality of the gas and solid temperatures. Combined heat and mass transfer in a single adsorbent grain coupled with water adsorption were described by the following system of differential equations similar to those of [2]:

(a) the energy balance equation for a single adsorbent grain including the heat of adsorption:

$$\rho_s C_p(T,N,x)\frac{\partial T}{\partial t} - \rho_s \Delta H \frac{x}{\mu_{salt}}\frac{\partial N}{\partial t} = \lambda_p \Delta T \qquad 0 < r < R_p \tag{1}$$

with the relevant initial and boundary conditions

$$T(r,0) = T_0 \qquad \frac{\partial T(0,t)}{\partial r} = 0 \qquad \alpha_p(T_f - T(R_p,t)) = \lambda_p \frac{\partial T(R_p,t)}{\partial r} \tag{2}$$

where $C_p(T,N,x)$ is the effective heat capacity of the grain [11].The equilibrium uptake $N(T,P_w)$ [mole H_2O/mole salt] at temperature T and pressure P_w was calculated by the approximation equations reported in [12].

(b) the mass balance equation including the diffusion of water vapour inside the grain and sorption processes:

$$\frac{\partial C_w}{\partial t} = D_e \Delta C_w - \frac{\rho_s x}{\mu_{salt}\varepsilon}\frac{\partial N}{\partial t} \tag{3}$$

(c) the ideal gas law:

$$P_w(r,t) = RT(r,t)C_w(r,t). \tag{4}$$

For the experiments analyzed the boundary conditions can be written as

$$C_w(R_p,t) = \frac{P_2(t)}{RT(R_p,t)}. \qquad \frac{\partial C_w(0,t)}{\partial r} = 0 \tag{5}$$

The total mass balance in the buffering and measuring reservoirs can be written as

$$\frac{P_1(t)V_1}{RT} + \frac{P_2(t)V_2}{RT} + m(t) = \frac{P_1(0)V_1}{RT} + \frac{P_2(0)V_2}{RT} + m(0) \tag{6}$$

where $m(t)$ is the mass of water adsorbed by the time t.
It is convenient to introduce the dimensionless water uptake χ as

$$\chi = \frac{(m(t) - m(0))}{(m(\infty) - m(0))}. \tag{7}$$

3. Particular features of the dynamic modeling at the initial stage of the adsorption process

The pressure in the whole volume became equalized for $t < 1$ s as a result of the vapour expansion from the buffering to measuring reservoirs accompanied by its simultaneous adsorption in the

measuring cell [3]. Accurate analysis of the process at $t < 1$ s has to be performed by considering the molar vapour flux J through the hole which connects the two reservoirs

$$\frac{V_1 dP_1}{RT\,dt} = -J$$
$$\frac{V_2 dP_2}{RT\,dt} + \frac{dm}{dt} = J \quad (8)$$

where $\frac{dm}{dt}$ can be calculated from Eqs. (1)–(5). The flux J from a reservoir at $P_1(t)$ to a reservoir at $P_2(t)$ can be calculated as [13]:

$$J = \frac{0.04 s P_1(t)}{\mu_w \sqrt{T}} \text{ when } P_1(t) > 2P_2(t)$$
$$J = \frac{0.08 s \sqrt{(P_1(t) - P_2(t))P_2(t)}}{\mu_w \sqrt{T}} \text{ when } P_1(t) < 2P_2(t) \quad (9)$$

where s is the area of the connecting hole (s was assumed to be 1 cm^2). The numerical analysis of Eqs. (1)–(9) made for SWS-1L revealed that under the experimental conditions of [3] the pressures became equal in some 0.01 s. As water adsorption on the initially dry grains was very fast, the uptake reached 0.06 g/g by the first second of the process [3] that has to be taken into consideration when the efficient diffusivity and heat transfer coefficients are determined. The concordant solution of boundary-value problems (1)–(5) and integral Eq. (6) at various inflowing modes (8), (9) is obligatory for correct determination of these coefficients.

The system of Eqs. (1)–(9) was numerically solved by the method of runs and iterations including an implicit finite difference method in order to obtain distributions $T(r,t)$, $C_w(r,t)$ and, therefore, $P_w(r,t)$ and $N(r,t)$. An iso-volumetric discretisation in the radial direction was applied as it was done in [14]. The temporal evolution of pressures $P_1(t)$ and $P_2(t)$ as well as the dimensionless adsorption $\chi(t)$ were the final results of the modeling.

Another peculiarity of the modeling comes from the fact that the uptake change during the adsorption run was from $N_0 = 0.065$ to $N_f = 4.3$ mole H_2O per 1 mole $CaCl_2$. In this range the dependence of the uptake on the Polanyi sorption potential is highly non-linear and contains domains of a step-wise shape [12,15]. This dramatically impairs the convergence of iterative procedures and undesirably extends calculating time.

4. Analysis of the experimental data

Theoretical dependences of the vapour pressure and dimensionless uptake on time calculated with the selected values of $D = 6.0\ 10^{-6}\ m^2/s$ and $\alpha = 70\ W/(m^2\ K)$ are in excellent agreement with those measured in [3] (Fig. 1). It is easy to make sure that these uptake curves are not exponential.

These optimal values of D_e and α_p have been selected as a result of the following procedure: for each pair D_e and α_p the average squared error was calculated as $\sigma = \sqrt{\frac{\sum_{i=1}^{i=n}(\chi_{exp}(t_i) - \chi_{theory}(t_i, D_e, \alpha_p))^2}{n}}$, where $\chi_{exp}(t_i)$ is the experimental dimensionless uptake, $\chi_{theory}(t_i, D_e, \alpha_p)$ is the calculated dimensionless uptake, $n \approx 10^3$ is the number of data readings [3]. The graph of $\sigma(D_e, \alpha_p)$ function was a wrapped plane looking like a valley (Fig. 2) whose bottom corresponded to the selected D_e and α_p, the Pirson coefficient being equal to 0.998.

As selected optimal values of D_e and α_p agree well with those obtained in [2] although some difference does exist. Lower optimal D_e-value reported in [2] might be due to the fact that the model developed in [2] failed in describing S-shaped parts of the kinetic curves recorded within the first dozens of seconds. The approximation of the S-shaped experimental dependence by a convex calculated curve, when the temperature jump of the metal plate is abrupt, could lead to underestimating the efficient diffusivity. As a result, the efficient heat transfer coefficient was likely to be overestimated in [2]. We believe that the coefficients D_e and α_p obtained in this communication more accurately conform to the physical model of the adsorption process involved. This example once more confirms that a careful consideration of the initial adsorption stage is a matter of principle for correct description of the adsorption dynamics in both model and real AHP.

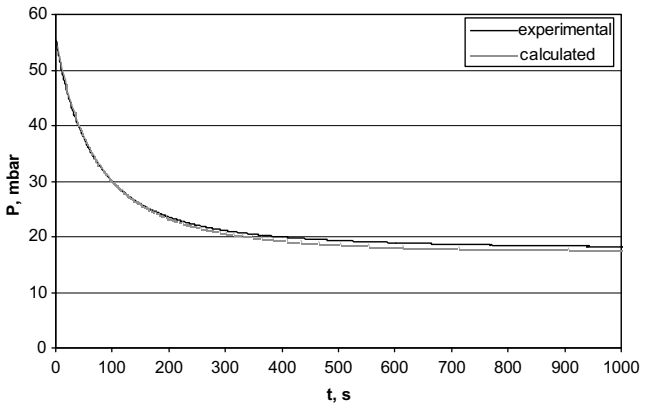

Fig. 1a. Experimental [3] and theoretical (calculated with the values of $D = 6.0 \times 10^{-6}\ m^2/s$ and $\alpha = 70\ W/(m^2\ K)$) dependences of the pressure vs time.

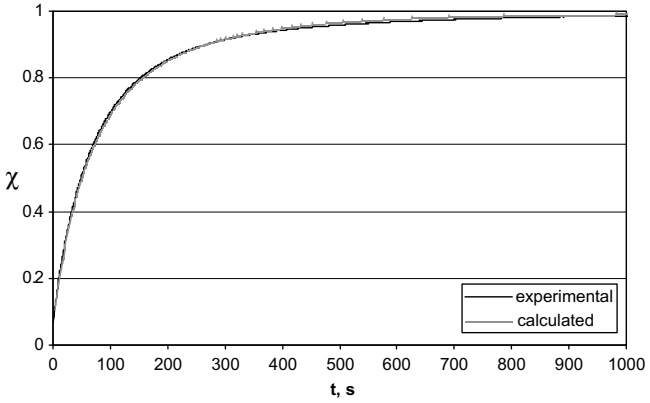

Fig. 1b. Experimental [3] and theoretical (calculated with the values of $D = 6.0 \times 10^{-6}\ m^2/s$ and $\alpha = 70\ W/(m^2\ K)$) dependences of the dimensionless uptake vs time.

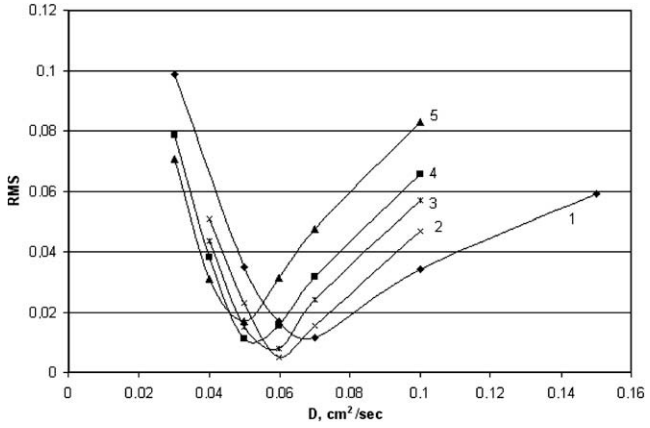

Fig. 2. The average squared error of the calculated and experimental curves as a function of D_e at various values of α_p: 1–60 W/(m² K), 2–70 W/(m² K), 3–80 W/(m² K), 4 –90 W/(m² K), 5–120 W/(m² K).

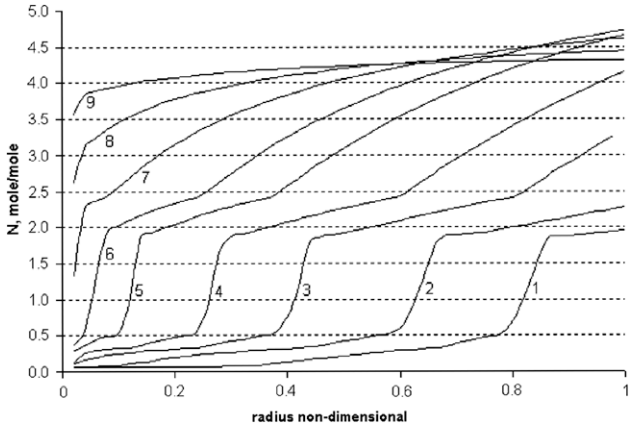

Fig. 3. Radial profiles of the water concentrations in the adsorbed state at various times (in seconds): 1–3.11, 2–11.1, 3–25.1, 4–50.6, 5–100.6, 6–150.3, 7–250.2, 8–400.9 and 9–601,7. 0 on the *X*-axis indicates the grain centre, 1 – the grain external surface.

Using these optimal values of D_e and α_p radial profiles of the grain temperature, the water concentrations in the adsorbed and gas phases were calculated as a function of time.

The shape of the uptake distribution was quite complex and contained steeps and quasi-plateas (Fig. 3) which closely resemble the shape of the equilibrium curve of water adsorption on SWS-1L [12,15] between the boundary uptakes $N = 0.065$ and $N = 4.30$ ([12,15]). This reveals the strong interrelationship between the shapes of the water sorption isotherm and the radial uptake profile.

The average uptake is plotted vs the average grain temperature in Fig. 4a; starting point A corresponds to $N_0 = 0.065$ mole/mole and $T_{av} = 50$ °C. The initial rate of adsorption was very high that resulted in a fast quasi-adiabatic heating of the grain up to 98 °C. Then the grain was getting cold until it reached the equilibrium point B at $N = 4.3$ mole/mole and $T_{av} = 50$ °C. It is worthy to mention that the surface uptake passed through a maximum at $t = 150$ s (Fig. 3) and was larger than the equilibrium one at point B. This resulted from the combined effect of the simultaneous falling of the both temperature and pressure along lines 1–9 in Fig. 4a.

A linear connection between the average grain temperature and the uptake (Fig. 4a) indicated that for the first two seconds the heating is nearly adiabatic. The grain temperature rise estimated under purely adiabatic conditions was 44 °C that is close to the experimentally recorded.

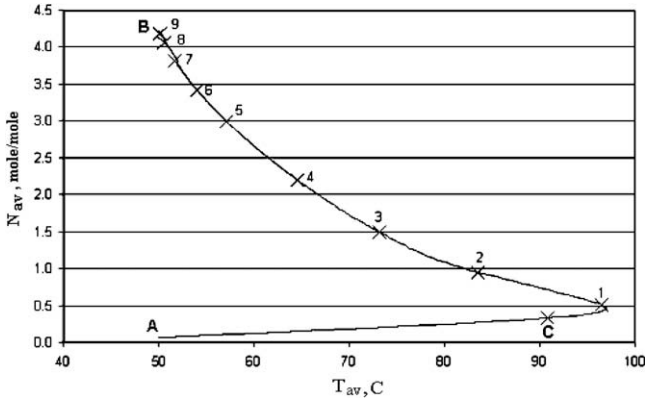

Fig. 4a. Evolution of the average grain temperature T_{av} vs average uptake N_{av}. Numbers 1–9 correspond to the same times as in Fig. 3. Point C corresponds to $t = 1$ s.

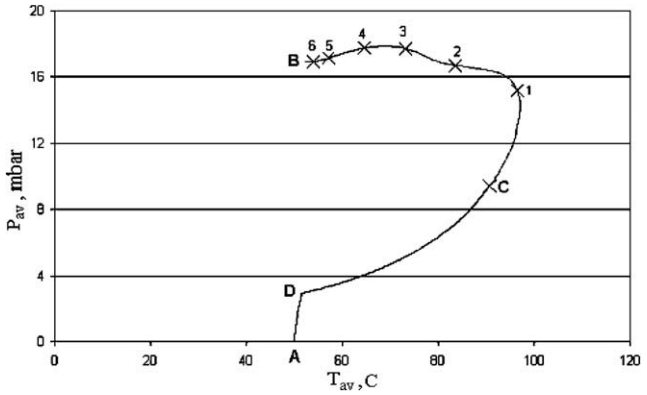

Fig. 4b. Evolution of the average grain temperature T_{av} vs the average pressure inside the grain P_{av}. Point A corresponds to the initial state of the system, point B to the end of the adsorption process. Notations are the same as in Fig. 3.

The average pressure is plotted vs the average grain temperature in Fig. 4b. The initial pressure jump (point D) was due to the vapour expansion from the buffering to measuring reservoirs accompanied by its simultaneous adsorption in the measuring cell. Then the fast growth of the both temperature and pressure was observed. Along fragment 1–3 the grain was getting cold, however the pressure inside the grain continued increasing due to the water diffusion through the external grain surface.

The radial distribution of temperature was almost uniform at $t > 1$ s (Fig. 5a), means along lines 1–9 in Fig. 4a when the grain was getting cool. At very short times a large temperature gradient

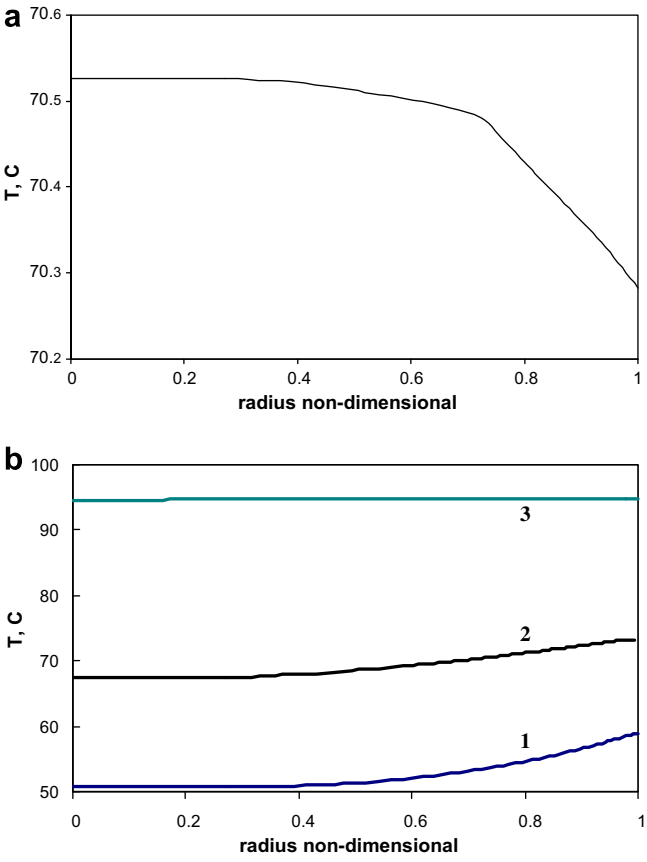

Fig. 5. The radial distribution of temperature. (a) $t = 31.4$ s and (b) curve 1 – $t = 0.07$ s, curve 2–0.15 s, curve 3–1 s.

along the grain was found (Fig. 5b) that is a quite rare case as commonly an adsorbent grain is assumed to have a uniform temperature distribution due to its sufficiently large thermal conductivity [5]. The reason of this non-isothermal behaviour at the very beginning of the process was the extremely fast water adsorption on the external grain surface initiated by the large pressure jump.

5. Resume

The mathematical model of the coupled heat and mass transfer in the course of water adsorption on a single adsorbent grain, which is in thermal contact with an isothermal metal plate has been presented. Adsorption was caused by a large jump of the vapour pressure over the grain as measured in [3]. The vapour expansion from the buffering to measuring reservoirs accompanied by its simultaneous adsorption in the measuring cell was also taken into account. As the water adsorption on the initially dry grains was very fast, the uptake reached 0.06 by the first second of the process that has to be taken into consideration when the efficient diffusivity and heat transfer coefficients are determined. The concordant solution of boundary-value problems (1)–(5) and integral Eq. (6) at various inflowing modes (8), (9) is obligatory for correct determination of these coefficients.

The radial profiles of the grain temperature as well as water concentrations in the adsorbed and gas phases were calculated as a function of time. Strong interrelationship between the shapes of the water sorption isotherm and the radial uptake profile was revealed. The best fit to the experimental data of [3] corresponds to the water diffusivity $D_e = 6.0 \times 10^{-6}\ m^2/s$ and the coefficient of the heat transfer $\alpha_p = 70\ W/(m^2\ K)$ which are larger than those measured in quasi-equilibrium experiments.

Acknowledgments

The authors thank the Russian Foundation for Basic Researches (projects 08-08-00808 and 07-08-13620) for partial financial support.

References

[1] Yu.I. Aristov, B. Dawoud, I.S. Glaznev, A. Elyas, A new methodology of studying the dynamics water sorption/desorption under real operating conditions of adsorption heat pumps: Experiment, Int. J. Heat Mass Transfer 51 (19–20) (2008) 4966–4972.
[2] B.N. Okunev, A.P. Gromov, L.I. Heifets, Yu.I. Aristov, A new methodology of studying the dynamics of water sorption/desorption under real operating conditions of adsorption heat pumps: modelling of coupled heat and mass transfer in a single adsorbent grain, Int. J. Heat Mass Transfer 51 (1-2) (2008) 246–252.
[3] B. Dawoud, Yu. I. Aristov, Experimental study on the kinetics of water vapour sorption on selective water sorbents, silica-gels and alumina under typical operating conditions of sorption heat pumps, Int. J. Heat Mass Transfer 46 (2) (2003) 273–281.
[4] L. Schnabel, H.-M. Henning, Experimental and simulation study on the kinetics of water vapor adsorption on different kinds of adsorptive material matrices, in: Proceedings of the International Conference on Sorption Heat Pumps, ISHPC05, June 22–24, Denver, CO, USA, Paper no. 39 (2005) pp. 1–8.
[5] D.M. Ruthven, Principles of Adsorption and Adsorption Processes, John Wiley and sons, New York, 1984.
[6] A. Brunovska, V. Hlavacek, J. Ilavsky, J. Valtyni, An analysis of nonisothermal one-component sorption in a single adsorbent particle, Chem. Eng. Sci. 33 (1978) 1385.
[7] A. Brunovska, V. Hlavacek, J. Ilavsky, J. Valtyni, Non isothermal one component sorption in a single adsorbent particle effect of external heat transfer, Chem. Eng. Sci. 35 (1980) 757.
[8] R. Haul, H. Stremming, Nonisotermal sorption kinetics in porous adsorbents, J. Colloid Interface Sci. 97 (1984) 348.
[9] L.M. Sun, F. Meunier, A detailed model for non-isothermal sorption in porous adsorbents, Chem. Eng. Sci. 42 (1987) 1585.
[10] E. Yamamoto, F. Watanabe, N. Kobayashi, M. Hasatani, Intraparticle heat and mass transfer characteristics of water vapor adsorption, J. Chem. Eng. Jpn. 35 (1) (2002) 1–8.
[11] Yu.I. Aristov, M.M. Tokarev, G. Cacciola, G. Restuccia, Specific heat and thermal conductivity of aqueous solutions of calcium chloride in silica pores, Russ. J. Phys. Chem. 71 (3) (1997) 391–394.
[12] M.M. Tokarev, B.N. Okunev, M.S. Safonov, L.I. Heifets, Yu.I. Aristov, Approximation equations for describing the sorption equilibrium between water vapor and a $CaCl_2$-in-silica gel composite sorbent, Russ. J. Phys. Chem. 79 (9) (2005) 1490–1494.
[13] L.G. Loytsyansky, Mechanics of liquid and gas, Nauka, Moscow, 1978 (Russian).
[14] L.M. Sun, Y. Feng, M. Pons, Numerical investigation of adsorptive heat pump systems with thermal wave heat regeneration under uniform-pressure conditions, Int. J. Heat Mass Transfer 40 (2) (1997) 281–293.
[15] Yu.I. Aristov, M.M. Tokarev, G. Cacciola, G. Restuccia, Selective water sorbents for multiple applications: 1. $CaCl_2$ confined in mesopores of the silica gel: sorption properties, React. Kinet. Catal. Lett. 59 (2) (1996) 325–334.